COMMISSIONS G1 AND G4 OF THE IAU
INFORMATION BULLETIN ON VARIABLE STARS
Volume 63 Number 6241 DOI: 10.22444/IBVS.6241

Konkoly Observatory
Budapest
17 May 2018

HU ISSN 0374 – 0676

MULTICOLOR LIGHT CURVES AND PERIOD ANALYSIS OF IL Cnc

ALTON, K.B.

70 Summit Ave, Cedar Knolls, NJ, USA, email: kbalton@optonline.net

Abstract

The spectral type and orbital period were estimated from multicolor (B, V and I_c) ccd-based photometric observations acquired in 2014 and 2018. Period analysis from eclipse timing differences indicate that no significant change in the orbital period 0.267656 d has occurred since 2003.

IL Cnc (V=$12\overset{m}{.}6$; $08^h55^m51\overset{s}{.}507$ +20°03′38″.56 (epoch=J2000)) was first reported to be a W UMa-type variable star by Rinner et al. (2003) based on unfiltered ccd data. Photometric data were also collected from this system during the ROTSE-I survey (NSVS; Woźniak et al. 2004) and later captured by the ASAS Survey (Pojmański et al. 2005). Sparsely sampled light curve data acquired over the time span between 1999 and 2005 were folded by period analysis. This report describes the results from the first multicolor (BVI_C) ccd-based photometric study conducted on this variable target. The analysis of eclipse time differences (ETD) calculated from times-of-minima published in the literature and new data presented herein has resulted in an improved ephemeris for IL Cnc.

Time-series images were taken (90-sec) in 2014 with an SBIG ST-8XME CCD camera mounted at the Cassegrain focus of a 0.28-m catadioptric telescope. This f/6.4 instrument located in UnderOak Observatory (UO; NJ, USA) produces an image scale of 2.06″/px (bin=2×2) and a field-of-view (FOV) of 17.5′×26.3′. Image acquisition (raw lights, darks, and flats) at UO was performed as described elsewhere (Alton 2016) and produced at least 282 values in each bandpass (B,V and I_C). Similarly at Desert Bloom Observatory (DBO; AZ, USA), an SBIG STT-1603ME CCD camera mounted at the Cassegrain focus of a 0.4-m catadioptric telescope was used for imaging IL Cnc in 2018. This f/6.8 instrument produces an image scale of 1.36″/px (bin=2×2) and a FOV of 11.5′×17.2′. At DBO, image acquisition (75-sec) was performed using MaxIm DL Version 6.13 (Diffraction Limited) or TheSkyX Pro Version 10.5.0 (Software Bisque). This most recent imaging campaign produced at least 235 individual photometric values in each bandpass. Both ccd cameras were equipped with B, V and I_C filters manufactured to match the Johnson-Cousins-Bessell prescription. Calibration and registration of all images collected at UO and DBO were performed with AIP4Win v2.4.0 (Berry and Burnell 2005). Instrumental readings were reduced to catalog-based magnitudes using the reference MPOSC3 star fields (Warner 2007) built into MPO Canopus v10.7.1.3 (Minor Planet Observer). The 2014 and 2018 light curves (LC) used an identical ensemble of five non-varying comparison stars in the same FOV. The identity, J2000 coordinates and color index ($B-V$) of these stars are listed in Table 1. Only data from images taken above 30° altitude (airmass <2.0) were accepted in order to minimize error due to differential refraction and color extinction.

Table 1. FOV identity, name, coordinates and color index ($B-V$) for the target (T) and comparison stars (1-5) used for ensemble aperture photometry.

FOV Identity	Name	$\alpha_{2000.0}$ hh:mm:ss	$\delta_{2000.0}$ $^\circ$ $'$ $''$	MPOSC3 $(B-V)$
1	GSC 01400-0523	08 56 04.26	+20 00 08.2	0.560
2	GSC 01400-0279	08 56 04.97	+20 01 06.8	0.711
3	GSC 01400-0330	08 56 11.63	+20 09 37.5	0.652
4	GSC 01400-0161	08 55 35.04	+20 05 05.6	0.588
5	GSC 01400-0406	08 55 34.19	+20 08 21.6	0.557
T	IL Cnc	08 55 51.51	+20 03 38.6	0.983

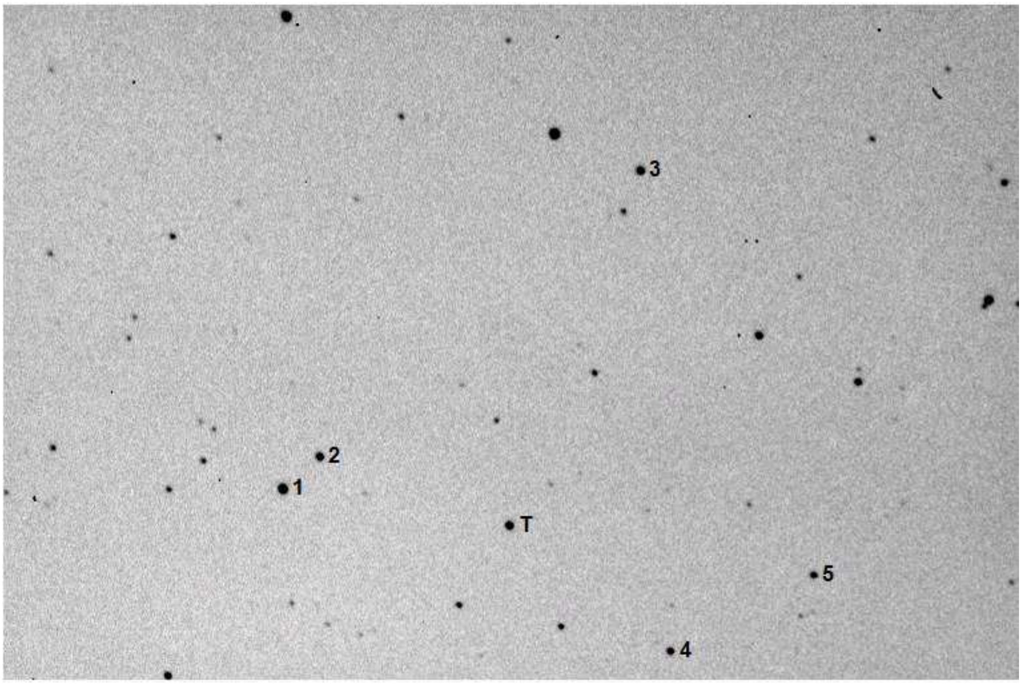

Figure 1. Observed field-of-view for IL Cnc (T) obtained at UO. The comparison stars are marked according to the numbers (1-5) assigned in Table 1.

Sparsely sampled LC data from the ROTSE–I (1999–2000) and ASAS surveys (2002–2005) were adjusted to the same average magnitude and subjected to period analysis using the ANOVA routine proposed by Schwarzenberg-Czerny (1996) and implemented within Peranso v2.5 (Vanmunster 2006). The period-folded ($P = 0.267656 \pm 0.000009$ d) results (Fig. 2) indicate that significant differences in the brightness at maximum and minimum light can occur.

Photometric data from 2014 (Fig. 3) and 2018 (Fig. 4) could be folded using an identical period solution (0.267656 ± 0.000001 d) derived by Fourier analysis (FALC; Harris et al. 1989). This period was independently verified using ANOVA (Schwarzenberg-Czerny 1996). Nine new times-of-minima (ToM) were calculated using the method of Kwee and van Woerden (1956). A mean ToM value was calculated for each night time session since no obvious color dependency (BVI_C) was observed. These are summarized in Table 2 along with other published ToM values dating back to 2003. Cycle number and ETD values were calculated from the reference ephemeris (Rinner et al. 2003) where:

$$HJD_0 = 2452721.5705 + 0\overset{d}{.}26765 \times E.$$

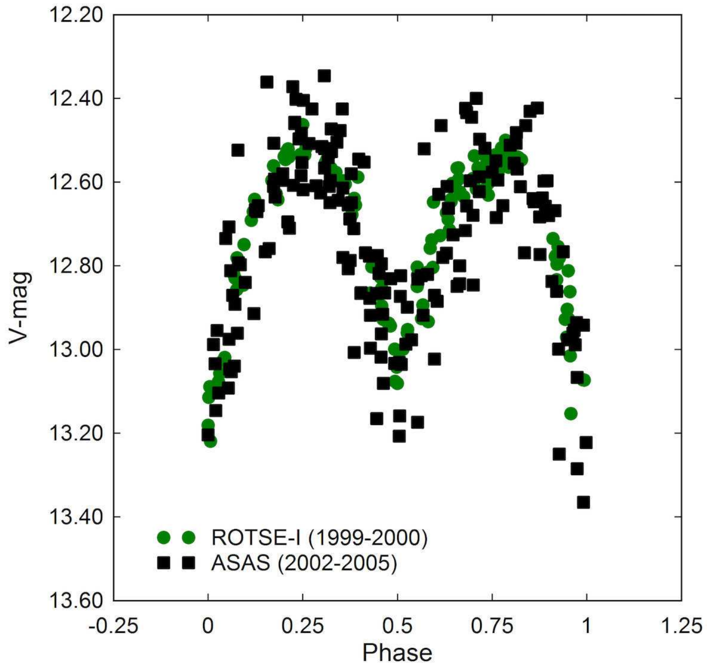

Figure 2. Folded ($P = 0.267656 \pm 0.000009$ d) light curves (V-mag) for IL Cnc produced from the ROTSE–I and ASAS Surveys.

Regression analysis of the ETD values calculated from all the observed and predicted minimum times versus the period cycle number produced a straight-line relationship indicating that the orbital period for this system does not appear to have substantially changed since 2003 (Fig. 5). These data lead to an improved linear ephemeris:

$$HJD = 2458131.9657(9) + 0.2676559(1) \times E.$$

It is clear from the steep slope of the ETD vs. epoch plot represented in Fig. 5, that the initial estimate for the orbital period (P=0.26765 d) was not sufficiently accurate, otherwise the data would have fallen on a line nearly parallel to the x-axis. If one were to substitute the improved value (P=0.2676559 d) for the original value reported by Rinner et al. 2003, then the resulting linear fit would illustrate this effect (Fig. 6). Since all but the first value represents data collected over a relative short time span (≈ 10 y), it is far too early to establish whether some underlying periodicity may remain hidden in the data. Additional ToMs will be necessary to more thoroughly examine the secular behavior of this system.

The multicolor LCs (BVI_C) for IL Cnc shown in Fig. 3 (2014) and Fig. 4 (2018) exhibit a shape characteristic of an eclipsing W UMa-type binary system. Peak asymmetry is observed in the 2018 LCs during maximum light such that Max II>Max I whereas not as much difference was observed at quadrature in 2014. This behavior, also called the O'Connell effect (O'Connell 1951), is generally attributed to hot or cold spots which can be large enough to affect the brightness in localized regions of either star. W UMa-type overcontact systems are well known to be photospherically active and from year-to-year can show large differences in maximum and minimum light. LC data collected from IL Cnc during the ASAS Survey dramatically illustrate this effect particularly during Min I and Max II (Fig. 2). No high resolution classification spectrum is available for IL Cnc, however an estimate from (B–V) and (V–I_C) color indices generated from the new LCs herein

Table 2. Eclipse time differences (ETD) calculated from published times-of-minima for IL Cnc along with eight new values reported for the first time in this study.

HJD (ToM) -2400000	Error	ETD	Cycle Number	Minimum type	Reference
52721.5705	-	0.000	0	primary	Rinner et al. (2003)
54500.4124	0.0004	0.04000	6646	primary	Hübscher et al. (2010)
54831.9068	0.0009	0.04987	7884.5	secondary	Diethelm (2009)
54866.4299	0.0003	0.04613	8013.5	secondary	Hübscher and Monninger (2011)
55245.8286	0.0009	0.05095	9431	primary	Diethelm (2010)
55275.4110	0.0013	0.05802	9541.5	secondary	Hübscher and Monninger (2011)
55295.3479	0.0010	0.05500	9616	primary	Hübscher and Monninger (2011)
55295.4840	0.0009	0.05727	9616.5	secondary	Hübscher and Monninger (2011)
55523.9260	0.0002	0.06000	10470	primary	Nelson (2011)
55571.8365	0.0003	0.06115	10649	primary	Diethelm (2011)
55571.9700	0.0003	0.06083	10649.5	secondary	Diethelm (2011)
55627.3762	0.0002	0.06347	10856.5	secondary	Hübscher and Lehmann (2012)
55667.6576	0.0004	0.06355	11007	primary	Diethelm (2011)
56000.6190	0.0040	0.06835	12251	primary	Diethelm (2012)
56000.7575	0.0007	0.07302	12251.5	secondary	Diethelm (2012)
56355.6678	0.0002	0.07943	13577.5	secondary	Nelson (2014)
56643.5313	0.0001	0.08585	14653	primary	Hübscher (2014)
56677.7910	0.0002	0.08585	14781	primary	Nelson (2015)
56711.6489	0.0003	0.08602	14907.5	secondary	This study
56714.5936	0.0003	0.08656	14918.5	secondary	This study
56719.1427	0.0002	0.08601	14935.5	secondary	This study
56720.6151	0.0006	0.08568	14941	primary	This study
56732.5252	0.0005	0.08562	14985.5	secondary	This study
56743.3679	0.0011	0.08850	15026	primary	Hübscher and Lehmann (2015)
56743.5003	0.0011	0.08707	15026.5	secondary	Hübscher and Lehmann (2015)
57414.3818	0.0005	0.10385	17533	primary	Hübscher (2017)
57414.5167	0.0007	0.10492	17533.5	secondary	Hübscher (2017)
58129.8257	0.0002	0.11824	20206	primary	This study
58130.8961	0.0002	0.11913	20210	primary	This study
58131.8318	0.0001	0.11801	20213.5	secondary	This study
58131.9667	0.0002	0.11910	20214	primary	This study

and those reported by four other surveys (USNO-B1, 2MASS, SDSS-DR9 and UCAC4) cataloged in VizieR (Lasker et al. 1996) suggests that it is an early K type system. This assignment is supported by a recent publication (Qian et al. 2017) in which low resolution (R $\approx$ 1800) spectra were obtained from over 7900 stars; therein IL Cnc is classified as a main sequence K3 system. Nonetheless, additional high resolution spectroscopic data may be required to unequivocally classify this system. Attempts to model these data with PHOEBE 0.31a (Prša and Zwitter 2005), a GUI front-end to the Wilson-Devinney code (Wilson and Devinney 1971), failed to produce a unique solution for the mass-ratio since IL Cnc only exhibits a partial eclipse ($i \approx 74°$). As such any photometric solution will suffer from degeneracy while trying to simultaneously optimize orbital inclination (i) and mass-ratio (q_{ph}) unless there is a total eclipse (Terrell and Wilson 2005). This behavior is manifestly confirmed (Fig. 7) during a procedure called "q-search" or "grid-search" to find a best value for the mass-ratio. Essentially q is incrementally changed within a fixed interval during Roche modeling while the orbital inclination (i), surface potential of the primary (Ω_1) and effective temperature of the secondary (T_2) were allowed to vary during optimization by differential corrections to minimize χ^2. As can be seen (Fig. 7) there is essentially no meaningful difference in the curve fits when q_{ph} varies between 1.5 and 2. In this case it is evident that radial velocity data will be necessary to produce an accurate mass-ratio and Roche model for IL Cnc.

In summary, LC and eclipse timing data for IL Cnc has revealed a W UMa-type system in which the orbital period has not meaningfully changed since 1999. A preliminary classification of IL Cnc based on color index $(B–V)$ and $(V–I_C)$ and low resolution spectroscopic data suggests that the primary component is an early K-type star. A comparison of LCs produced from photometric data collected during the ROTSE-I and ASAS surveys along with those new data reported herein suggest that IL Cnc has an active photosphere like most other overcontact binary systems possessing a strong magnetic dynamo. Due to limitations imposed by a partial eclipse, it is not possible to derive a reliable value for the mass-ratio for this system without supporting radial velocity data.

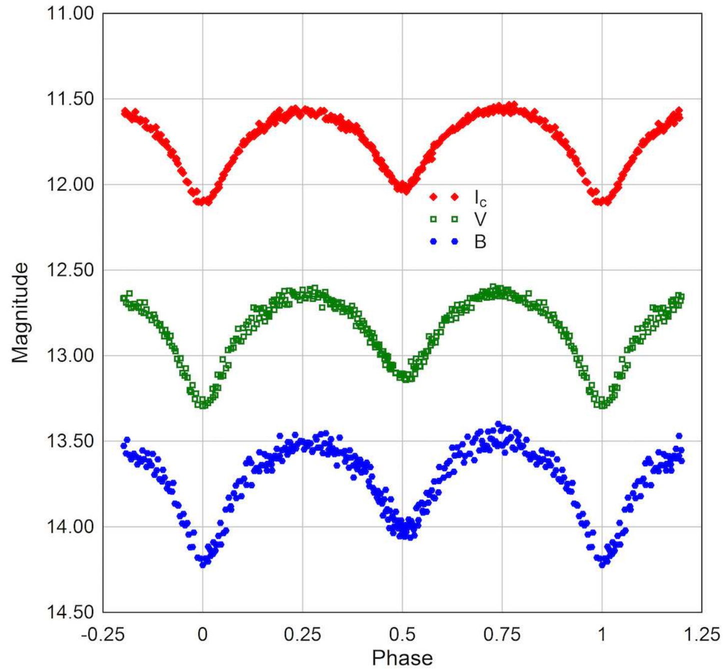

Figure 3. Folded $(P = 0.267656 \pm 0.000001$ d) light curves (BVI_C) for IL Cnc produced at UnderOak Observatory in 2014

Acknowledgments: This research has made use of the SIMBAD and VizieR databases, operated at Centre de Données astronomiques de Strasbourg, France. In addition, the International Variable Star Index maintained by the AAVSO, the ASAS Catalogue of Variable Stars and the Northern Sky Variability Survey were mined for valuable information. The diligence and dedication of all associated with these organizations is greatly appreciated. Many thanks to the anonymous referee who provided valuable feedback on this report.

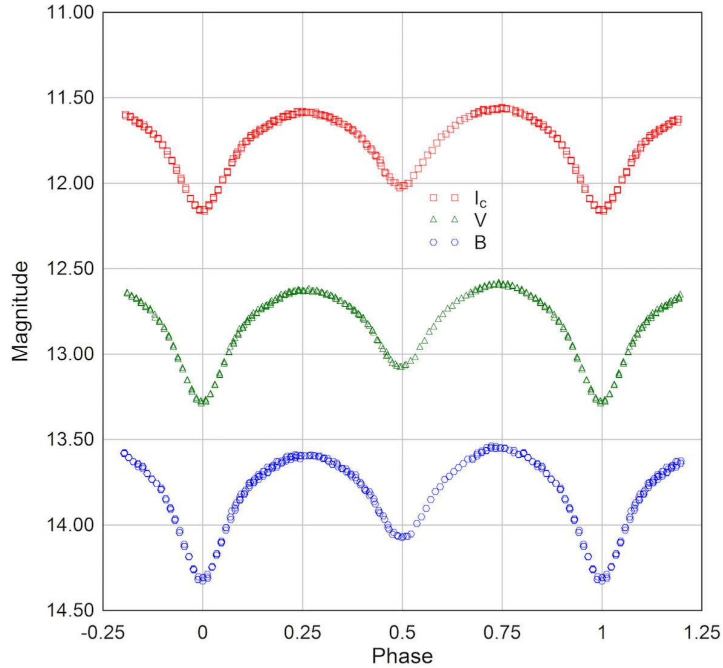

Figure 4. Folded ($P = 0.267656 \pm 0.000001$ d) light curves (BVI_C) for IL Cnc produced at Desert Bloom Observatory in 2018

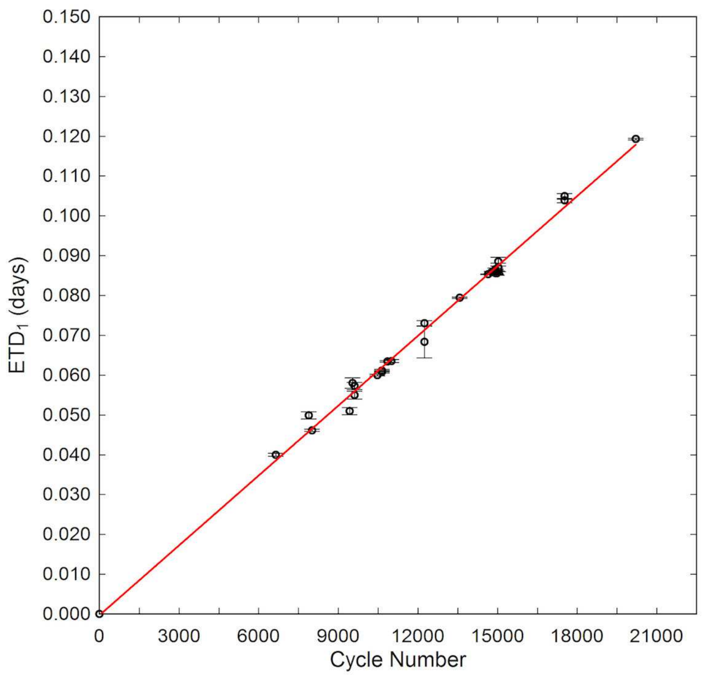

Figure 5. Linear ephemeris for IL Cnc determined from eclipse timing differences observed between 2003 and 2018 using the period ($P = 0.26765$ d) defined by Rinner et al. 2003

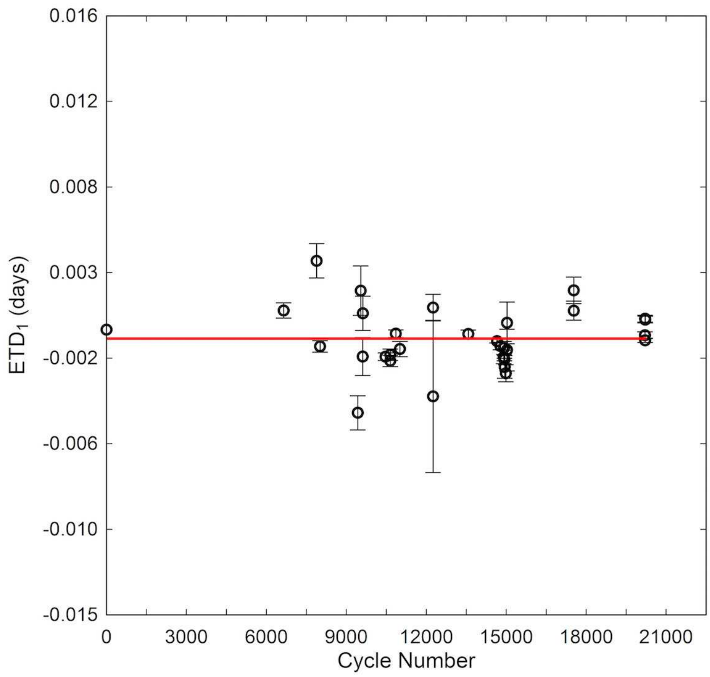

Figure 6. Linear ephemeris for IL Cnc determined from eclipse timing differences observed between 2003 and 2018 using the improved value for orbital period ($P = 0.2676559 \pm 0.0000001$d)

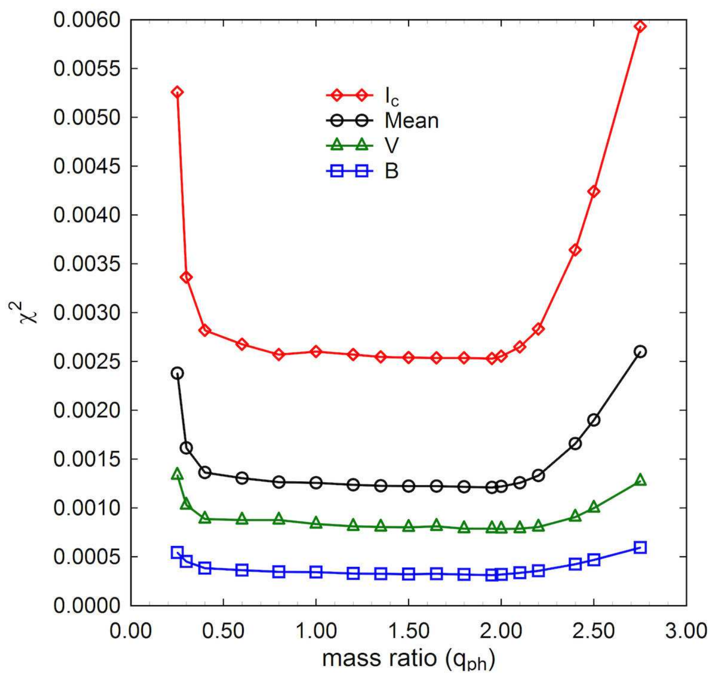

Figure 7. Results from q-search illustrating failure to find a unique value for the photometric mass-ratio (q_{ph}) where the best LC model fit reaches a distinct minimum error (χ^2)

References:

Alton, K.B., 2016, *JAAVSO*, **44**, 87

Berry, R. and Burnell, J., 2005, *The Handbook of Astronomical Image Processing*, 2nd Ed, Richmond VA, Willmann-Bell

Diethelm, R., 2009, *IBVS*, **5959**

Diethelm, R., 2010, *IBVS*, **5945**

Diethelm, R., 2011, *IBVS*, **5992**

Diethelm, R., 2012, *IBVS*, **6029**

Harris, A.W., Young, J.W., Bowell, E., et al., 1989, *Icarus*, **77**, 171 DOI

Hübscher, J., 2014, *IBVS*, **6118**

Hübscher, J., 2017, *IBVS*, **6196** DOI

Hübscher, J. and Lehmann, P.B., 2012, *IBVS*, **6026**

Hübscher, J. and Lehmann, P.B., 2015, *IBVS*, **6149**

Hübscher, J., Lehmann, P.B., Monninger, G., et al., 2010, *IBVS*, **5918**

Hübscher, J. and Monninger, G., 2011, *IBVS*, **5871**

Kwee, K.K. and Woerden, H. van, 1956, *BAN*, **12**, 327

Lasker, B.M., Sturch, C.R., Lopez, C., et al., 1996, *VizieR Online Data Catalog, Version 1.1*

Nelson, R.H., 2011, *IBVS*, **5966**

Nelson, R.H., 2014, *IBVS*, **6092**

Nelson, R.H., 2015, *IBVS*, **6131**

O'Connell D.J.K., 1951, *Pub. Riverview College Obs.*, **2**, 85

Qian, S.-B., He, J.-J., Zhang, J., et al., 2017, *Research in Astron. Astrophys.*, **17**, 087 DOI

Pojmański, G., Pilecki, B., Szczygiel, D., 2005, *AcA*, **55**, 275

Prša, A., and Zwitter, T., 2005, *ApJ*, **628**, 426 DOI

Rinner, C., Starkey, D. Demeautis, Ch., et al., 2003, *IBVS*, **5428**

Schwarzenberg-Czerny, A., 1996, *ApJ*, **460**, L107 DOI

Terrell, D. and Wilson, R.E., 2005, *ApSS*, **296**, 221 DOI

Vanmunster, T., 2006, *Peranso v2.5, Perios Analysis Software*, CBA Belgium Observatory

Warner, B. 2007, *Minor Planet Bulletin*, **34**, 113

Wilson, R. E. and Devinney, E. J., 1971, *ApJ*, **166**, 605 DOI

Woźniak, P.R., Vestrand, W.T. Akerlof, C.W., et al., 2004, *AJ*, **127**, 2436 DOI